First-principles GW-BSE excitations in organic molecules

Murilo L. Tiago$^{(a)*}$ and James R. Chelikowsky$^{(a,b)}$

$^{(a)}$ *Department of Chemical Engineering and Materials Science,*

Institute for the Theory of Advanced Materials in Information Technology,

Digital Technology Center, University of Minnesota, Minneapolis, MN 55455, USA.

$^{(b)}$ *Departments of Physics and Chemical Engineering,*

Institute for Computational Engineering and Science,

University of Texas, Austin, TX 78712, USA.

(Dated: November 23, 2018)

Abstract

We present a first-principles method for the calculation of optical excitations in nanosystems. The method is based on solving the Bethe-Salpeter equation (BSE) for neutral excitations. The electron self-energy is evaluated within the GW approximation, with dynamical screening effects described within time-dependent density-functional theory in the adiabatic, local approximation. This method is applied to two systems: the benzene molecule, C_6H_6, and azobenzene, $C_{12}H_{10}N_2$. We give a description of the photoisomerization process of azobenzene after an $n - \pi^\star$ excitation, which is consistent with multi-configuration calculations.

* corresponding author, Tel.: +1 512 232 2085, fax: +1 512 471 8694

I. INTRODUCTION

Predicting many-body excitations of weakly correlated systems from first principles is important, both to help understand the behavior of known systems as well as to design novel materials and technological devices. The study of optical excitations in systems at nanoscale size has been accentuated by recent achievements in nanotechnology and the potential growth of the field [1, 2, 3]. On the theory side, time-dependent density functional theory in the adiabatic, local approximation (TDLDA) has been used to study a wide class of nanosystems ranging from organic molecules to semiconducting and metallic clusters (see *e.g.* [4] and references therein). Alternatively, optical excitations of atoms, small molecules and bulk materials have been studied from first principles by solving the Bethe-Salpeter equation (BSE) for electrons and holes [5]. In bulk materials, the BSE approach is known to fully describe excitonic effects, which are missing in TDLDA [5, 6]. In confined systems such as clusters and isolated molecules, the BSE approach is expected to be more accurate than TDLDA, but extensive comparisons of both methods have not been done so far due to the complexity of most numerical implementations of the BSE. One source of complexity is the explicit evaluation of the dielectric function of the system. Early implementations [5] use a Fourier expansion of the static dielectric function, with dynamical effects included via semi-empirical models or ignored altogether. More recent studies employ generalized plasmon-pole models in the description of dynamical screening [7]. Öğüt and collaborators [8] have presented a fully *ab initio* technique for the calculation of the static dielectric function in real space, leading to important simplifications compared to Fourier-expansion techniques.

We propose a formulation of the BSE method that avoids the explicit evaluation of the dielectric function. All the information about electronic screening is contained in the polarizability operator, which is calculated within TDLDA by solving a generalized eigenvalue problem [4, 9]. After numerical diagonalization, eigenvectors give the spatial dependence of the polarizability, while eigenvalues give its frequency (time) dependence. Both the electronic self-energy and electron-hole interaction kernel, which enter explicitly in the BSE, are computed directly from the TDLDA polarizability. Once the BSE is reduced to a generalized, frequency-dependent eigenvalue problem, it is numerically diagonalized. The resulting normal modes are associated to neutral, optical excitations of the electronic system.

II. THEORETICAL METHOD

The underlying description of the electronic system is obtained within density-functional theory (DFT). The Kohn-Sham equations are solved in real space. Degrees of freedom related to core electrons are excluded from the problem by using norm-conserving pseudopotentials. We start by expressing the random-phase approximation (RPA) polarizability operator in the space of Kohn-Sham eigenstates in the usual way:

$$P^0_{cv,c'v'}(\omega) = \frac{\delta_{c,c'}\delta_{v,v'}}{\omega - \omega_{cv} + i0^+} - \frac{\delta_{c,c'}\delta_{v,v'}}{\omega + \omega_{cv} - i0^+} \tag{1}$$

where ω_{cv} is the difference between two Kohn-Sham eigenvalues, $\varepsilon_c - \varepsilon_v$, and 0^+ denotes an arbitrarily small quantity. We assume $\hbar = 1$ and ignore spin indices for the sake of clarity. The case of spin-polarized systems require slight modifications in the formalism. Here, we denote occupied Kohn-Sham orbitals by v, v' and unoccupied (virtual) ones by c, c'. Generic orbitals are denoted by letters i, j, n. Appropriate occupation factors should be included in Eq. (1) if partially populated orbitals are present [9]. Within TDLDA, the polarizability is written in terms of eigenvalues $\{\omega_m\}$ and eigenvectors $\{F^m_{vc}\}$ of an effective eigenvalue problem [9],

$$\Pi_{cv,c'v'} = \sum_{vc,v'c',m} \left[\frac{F^{m\star}_{vc} F^m_{v'c'}}{\omega - \omega_m + i0^+} - \frac{F^m_{vc} F^{m\star}_{v'c'}}{\omega + \omega_m - i0^+} \right] . \tag{2}$$

Both polarizabilities can also be expressed in real space by including Kohn-Sham eigenvectors according to the rule

$$\{\mathcal{O}\}(\mathbf{r}, \mathbf{r}') = \sum_{ij,i'j'} u_i(\mathbf{r}) u_j^\star(\mathbf{r}') \{\mathcal{O}\}_{ij,i'j'} u_{i'}^\star(\mathbf{r}) u_{j'}(\mathbf{r}') . \tag{3}$$

One key quantity in solving the Bethe-Salpeter equation for optical excitations is the electronic self-energy Σ, which can be computed from first principles within the so-called GW approximation (GWA) [10, 11]. This method has been used in a number of different systems and at different levels of sophistication. At its lowest level, the self-energy is schematically evaluated as $\Sigma_0 = G_0 W_0$, where G_0 is the (DFT) Green's function and $W_0 = [1 - VP_0]^{-1}V$ is the screened Coulomb interaction, with V being the bare Coulomb interaction, $V(\mathbf{r}) = e^2/r$. In this implementation, we go beyond RPA and use the TDLDA polarizability, Eq. (2). Having in mind that Π and P_0 are related to each other via $\Pi^{-1} = P_0^{-1} - (V + f)$ [6, 12],

where f is the TDLDA interaction kernel, $f = \frac{\delta V_{xc}}{\delta n}$, one can arrive at this expression for the self-energy:

$$\Sigma(\omega') = i \int \frac{d\omega}{2\pi} e^{-i\omega 0^+} G_0(\omega' - \omega) \left[V + V\Pi(\omega)V + \frac{1}{2} V\Pi(\omega)f + \frac{1}{2} f\Pi(\omega)V \right] \quad . \tag{4}$$

In Eq. (4), the first term inside square brackets denotes the bare exchange (Hartree) contribution. The second term is the correlation part. The last two terms have vertex corrections. Some aspects of Eq. (4) should be pointed out:

1. The additional vertex terms are written in symmetrized form, so that the resulting self-energy is symmetric with the interchange of arguments. In many-body notation, $\Sigma(1, 2) = \Sigma(2, 1)$.

2. By ignoring the f kernel and evaluating the polarizability as $\Pi^{-1} = P_0^{-1} - V$, we recover the self-energy at Σ_0 level of approximation. Adding a f kernel in the polarizability amounts to enhanced screening, which is partially compensated by the inclusion of vertex terms.

3. The frequency dependence of the polarizability is known from Eq. (2). Plasmon pole models are not needed.

Numerically, matrix elements of the self-energy can be evaluated by expressing the quantities V, Π, f in representation of Kohn-Sham orbitals using Eq. (3) and evaluating the self-energy directly from Eq. (4). We do not impose self-consistency between polarizability, self-energy and Green's function.

Optical excitations can be obtained either from the singularities of the TDLDA polarizability in frequency domain, Eq. (2), or by solving the BSE. In the second case, we set up a generalized eigenvalue problem where the interaction kernel K is no longer of the form $K = V + f$ as in TDLDA, but given by $K = \frac{\delta(V_H + \Sigma)}{\delta G}$ [5]. From Eq. (4), this reduces to

$$K_{vc,v'c'} = [V]_{vc,v'c'} + \left[V + V\Pi V + \frac{V\Pi f}{2} + \frac{f\Pi V}{2} \right]_{vv',cc'} \quad . \tag{5}$$

With this kernel operator, the BSE is solved numerically using standard procedures. The term inside the first pair of square brackets should be ignored for spin-triplet excitations [5, 6].

Having a frequency-dependent kernel makes the BSE a non-standard eigenvalue equation. In periodic systems, dynamical effects were found to be negligible if one is interested in the linear optical spectrum. In finite systems, quantum confinement effects increase the strength of the interaction kernel, resulting in somewhat stronger but still limited dynamical effects (about 0.01 eV for the SiH_4 system)[5]. Although we ignore those effects in the present work, they can be included by evaluating polarizability and kernel at some frequency close to the actual excitation frequencies obtained by solving the BSE.

III. APPLICATIONS

A test case of the procedure above is the isolated benzene (C_6H_6) molecule. For this system, we have solved the Kohn-Sham equations on a regular grid, with grid spacing 0.4 a.u. (0.21 Å). Electronic wave-functions were required to vanish outside a sphere of radius 16 a.u. (8.47 Å), centered on the molecule. Carbon-carbon and carbon-hydrogen bond lengths were fixed at their experimental values. After including self-energy corrections, the ionization potential is found to be 9.30 eV, in good agreement with the experimental value of 9.3 eV [13]. Benzene has a negative electron affinity of -1.12 eV, measured in resonance scattering experiments [14], which is in excellent agreement with the calculated electron affinity of -1.11 eV. Here, the negative electron affinity is interpreted as energy of the E_{2u} resonant state of the anion, and not the lowest energy required to extract one electron from the anion (which is zero because the anion is unstable). We observed that the inclusion of vertex corrections together with a TDLDA polarizability is essential for an accurate prediction of the ionization potential and electron affinity of benzene. In fact, the Σ_0 approximation predicts those quantities to be 9.84 eV and -0.54 eV respectively. Defining a "HOMO-LUMO gap" as the difference between ionization potential and electron affinity, the present approach and the Σ_0 approach agree in the value of the gap: 10.4 eV. This is somewhat consistent with the observation by del Sole and collaborators [15], who conducted a similar analysis in bulk silicon and found significant shifts in the valence band maximum and conduction band minimum, but only small change in the energy gap.

The low-energy optical spectrum of this molecule is dominated by a $\pi - \pi^\star$ complex, which arises from transitions between the degenerate highest occupied molecular orbital (HOMO) and lowest unoccupied molecular orbital (LUMO). Table I shows a comparison between

TDLDA and BSE predictions for some excitations in the $\pi - \pi^\star$-complex. Although singlet transitions B_{1u}^1 and E_{1u}^1, which are the dominant ones in the low-energy part of the absorption spectrum, are equally well described by both methods, there is a small but well-defined blue shift of dark transitions B_{1u}^3 and B_{2u}^1 within TDLDA. With the exception of the E_{1u}^1 transition, excitation energies obtained by solving the BSE are typically underestimated with respected to measured quantities. The overall deviation between measured and calculated transition energies is 0.1 to 0.3 eV.

The absorption spectrum of benzene, Fig. 1, shows the bright E_{1u}^1 transition, at 7.0 eV. The low, flat feature in the 6.0-7.0 eV range is due to coupling between $\pi - \pi^\star$ transitions and vibrational modes [13, 16], and it is absent in the calculated spectra because of the assumed structural rigidity. Beyond 10 eV, a number of sharp features in the measured spectrum results from transitions involving Rydberg states [13, 17]. The limited numerical accuracy in that energy range prevents a detailed identification of such transitions in the calculated spectrum.

A more interesting system is the azobenzene ($C_{12}H_{10}N_2$) molecule. This molecule has attracted considerable attention recently due to exciting experiments of light-driven mechanical manipulation at nanoscale. Some of these experiments are: demonstration of light-driven manipulation of liquid droplets on an optically active surface [1]; energy conversion in a polymeric azobenzene chain [2]; synthesis of an azobenzene compound which exhibits hinge-like motion when photo-irradiated [3]. The basic phenomenon explored in these experiments is photo-isomerization: the structure of azobenzene is induced to change from a *trans*-azobenzene configuration (TAB) to a metastable *cis*-azobenzene configuration (CAB) upon absorption/emission of radiation with the appropriate frequency. On the theory side, the detailed structural distortion involved in the process has been subject of discussion. Early analyses based on a restricted configuration interaction (CI) calculation [18] indicated that photo-isomerization following excitation to the first excited state occurs via inversion of one nitrogen in the azo group, causing an increase of 120° in the C-C-N bond angle ("inversion path"). On the other hand, recent multi-configuration and TDLDA calculations [19, 20] indicate that the most favorable path is a torsion of the N-N bond around its axis, causing a 180° rotation of one phenyl group with respect to the other ("rotation path"). Diau has proposed an alternative "synchronous inversion path" that can also lead to photo-isomerization [21].

We have studied optical excitations in the isolated azobenzene molecule, in order to test the accuracy of the present BSE approach. Isomerization along the rotation path was simulated by initially fixing the CNNC dihedral angle and minimizing the DFT total energy of the system with respect to all other degrees of freedom. A sequence of configurations was then obtained for various choices of the dihedral angle ranging from 0° (CAB) to 180° (TAB), as discussed in [20]. The Kohn-Sham equations were solved on real space, using a boundary radius of 20 a.u. (10.58 $\mathring{A}$) and grid spacing 0.4 a.u. (0.21 $\mathring{A}$). At the equilibrium configuration, *trans*-azobenzene has ionization potential 8.5 eV [22], which is consistent with the corresponding values of 8.6 eV, obtained from GW with a self-energy given by Eq. (4).

The calculated potential energy of the system in its ground state and the two lowest excited states is shown in Fig. 2. At each configuration, the potential energy is computed as a sum of ground-state potential energy and excitation energy, the latter computed either within TDLDA or BSE. Calculated excitation energies for the CAB and TAB configurations are shown in Table II. Deviations between the BSE and experimental excitation energies are small, within 0.3 eV. The CAB $\pi\pi^\star$ excitation energy has larger deviation, of almost 0.8 eV, which may indicate a difficulty in the theoretical description of higher-energy excitations. On the other hand, excitation energies obtained within TDLDA are systematically lower than the ones obtained within BSE by more than 0.4 eV, and substantially different from measured excitation energies.

Figure 2 shows that, once the system absorbs radiation and is promoted to its first excited state at either CAB or TAB configurations, there is no energy barrier preventing fast relaxation to an intermediate configuration, with dihedral angle around 90°. From that configuration, the system can decay to ground state and relax back to either the CAB or TAB configurations. This mechanism allows $trans \longrightarrow cis$ or $cis \longrightarrow trans$ isomerization after excitation to state $n\pi^\star$ (the first excited state). Excitation to the second excited state is not found to induce isomerization, unless there is decay to state $n\pi^\star$, since the profile of potential energy is rather flat along the rotation path.

Photo-isomerization involving higher-order excited states, which has been observed in laboratory, can also be studied once four-particle and more complex excitations are included in the theory. Multi-configuration calculations [19, 23] indicate that an excited state composed of two electrons promoted from the HOMO to the LUMO has a barrier-less potential energy profile along the rotation path. That excited state is not accurately described within

either TDLDA or BSE approaches in the current two-particle approximation. Despite this limitation, excited states of azobenzene can be studied within the BSE approach or, to a lower level of accuracy, TDLDA.

IV. CONCLUSION

In summary, we have discussed a first-principles method for the calculation of optical excitations in nanosystems, with applications to two organic molecules: benzene and azobenzene. The method is based on solving the Bethe-Salpeter equation (BSE) for neutral excitations, with dynamical screening described within TDLDA. To our knowledge, this is the *first time* that optical excitations in organic molecules are calculated using Green's function-based methods. The approach is completely system-independent and it can also be used to study inorganic systems.

[1] K. Ichimura, S-K. Oh, and M. Nakagawa, Science 288 (2000) 1624.

[2] T. Hugel, N.B. Holland, A. Cattani, L. Moroder, M. Seitz, and H.E. Gaub, Science 296 (2002) 1103.

[3] Y. Norikane and N. Tamaoki, Organic Lett. 6 (2004) 2595.

[4] I. Vasiliev, S. Öğüt , and J.R. Chelikowsky, Phys. Rev. B 65 (2002) 115416.

[5] M. Rohlfing and S.G. Louie, Phys. Rev. B 62 (2000) 4927, and references therein.

[6] G. Onida, L. Reining, and A. Rubio, Rev. Mod. Phys. 74 (2002) 601.

[7] L.X. Benedict, A. Puzder, A.J. Williamson, J.C. Grossman, G. Galli, J.E. Klepeis, J-Y. Raty, and O. Pankratov, Phys. Rev B 68 (2003) 085310; T.A. Niehaus, M. Rohlfing, F. Della Sala, A. Di Carlo, and Th. Frauenheim, Phys. Rev. A 71 (2005) 022508.

[8] S. Öğüt , R. Burdick, Y. Saad, and J.R. Chelikowsky, Phys. Rev. Lett. 90 (2003) 127401.

[9] M.E. Casida, in *Recent Advances in Density-Functional Methods*, Part I, ed. D. P. Chong, World Scientific, Singapore, 1995, p. 155.

[10] M.S. Hybertsen and S.G. Louie, Phys. Rev. B 34 (1986) 5390; L. Hedin, Phys. Rev. 139 (1965) A796.

[11] W.G. Aulbur, L. Jönsson, and J.W. Wilkins, *Solid State Physics*, eds. F. Seitz, D. Turnbull, and H. Ehrenreich, vol. 54, Academic, New York, 2000, p. 1.

[12] W. Hanke, Adv. Phys. 27 (1978) 287.

[13] G. Herzberg, *Molecular Spectra and Molecular Structure*, vol. III, *Electronic Spectra and Electronic Structure of Polyatomic Molecules*, Van Nostrand, New York, 1966.

[14] P.D. Burrow, J.A. Michejda, and K.D. Jordan, J. Chem. Phys. 86 (1987) 9.

[15] R. del Sole, L. Reining, and R.W. Godby, Phys. Rev B 49 (1994) 8024.

[16] G.F. Bertsch, A. Schnell, and K. Yabana, J. Chem. Phys. 115 (2001) 4051.

[17] E.E. Koch and A. Otto, Chem. Phys. Lett. 12 (1976) 476.

[18] S. Monti, G. Orlandi, and P. Palmieri, Chemical Physics 71 (1982) 87.

[19] P. Cattaneo and M. Persico, Phys. Chem. Chem. Phys. 1 (1999) 4739; L. Gagliardi, G. Orlandi, F. Bernardi, A. Cembran, and M. Garavelli, Theor. Chem. Acc. 111 (2004) 363; A. Cembran, F. Bernardi, M. Garavelli, L. Gagliardi, and G. Orlandi, J. Am. Chem. Soc. 126 (2004) 3234; T. Ishikawa, T. Noro, and T. Shoda, J. Chem. Phys. 115 (2001) 7503.

[20] M.L. Tiago, S. Ismail-Beigi, and S.G. Louie, J. Chem. Phys. 122 (2005) 094311.

[21] E. W-G. Diau, J. Phys. Chem. A 108 (2004) 950.

[22] P. Natalis and J.L. Franklin, Int. J. Mass Spectrom. Ion Phys. 40 (1981) 35.

[23] T. Fujino, S.Yu. Arzhantsev, and T. Tahara, J. Phys. Chem. A 105 (2001) 8123.

[24] J.P. Doering, J. Chem. Phys. 51 (1969) 2866.

[25] I.K. Lednev, T.-Q. Ye, P. Matousek, M. Towrie, P. Foggi, F.V.R. Neuwahl, S. Umapathy, R.E. Hester, and J.N. Moore, Chem. Phys. Lett. 290 (1998) 68.

[26] T. Nägele, R. Hoche, W. Zinth, and J. Wachtveitl, Chem. Phys. Lett. 272 (1997) 489.

TABLE I: Excitation energies of the lowest-energy neutral excitations in benzene. The BSE excitation energies were obtained with a static kernel. Energies in eV.

		TDLDA	BSE	Exp. [24]
triplet	B_{1u}^3	4.5	3.6	3.9
singlet	B_{2u}^1	5.4	4.9	5.0
	B_{1u}^1	6.2	6.1	6.2
	E_{1u}^1	6.9-7.2	7.2	6.9

TABLE II: Excitation energies of the lowest-energy neutral excitations in azobenzene. Energies in eV.

		TDLDA	BSE	Exp.
TAB	$n\pi^\star$	2.1	2.5	2.80 [25]
	$\pi\pi^\star$	3.3	4.0	3.94 [25]
CAB	$n\pi^\star$	2.2	2.6	2.86 [26]
	$\pi\pi^\star$	3.2	3.6	4.38 [26]

Figures

Fig. 1 Absorption spectrum of benzene, calculated within TDLDA (upper panel) and BSE (lower panel). A Gaussian broadening of 0.15 eV was used below 10.0 eV, and 0.5 eV above that frequency. The measured spectrum [17] is shown in dashed lines.

Fig. 2 Potential energy of the isolated azobenzene molecule in its ground state and the two lowest spin-singlet states, obtained within TDLDA (upper panel), and BSE (lower panel). The molecular structure is schematically depicted at the two stable configurations (TAB and CAB) and one intermediate configuration along the isomerization path.
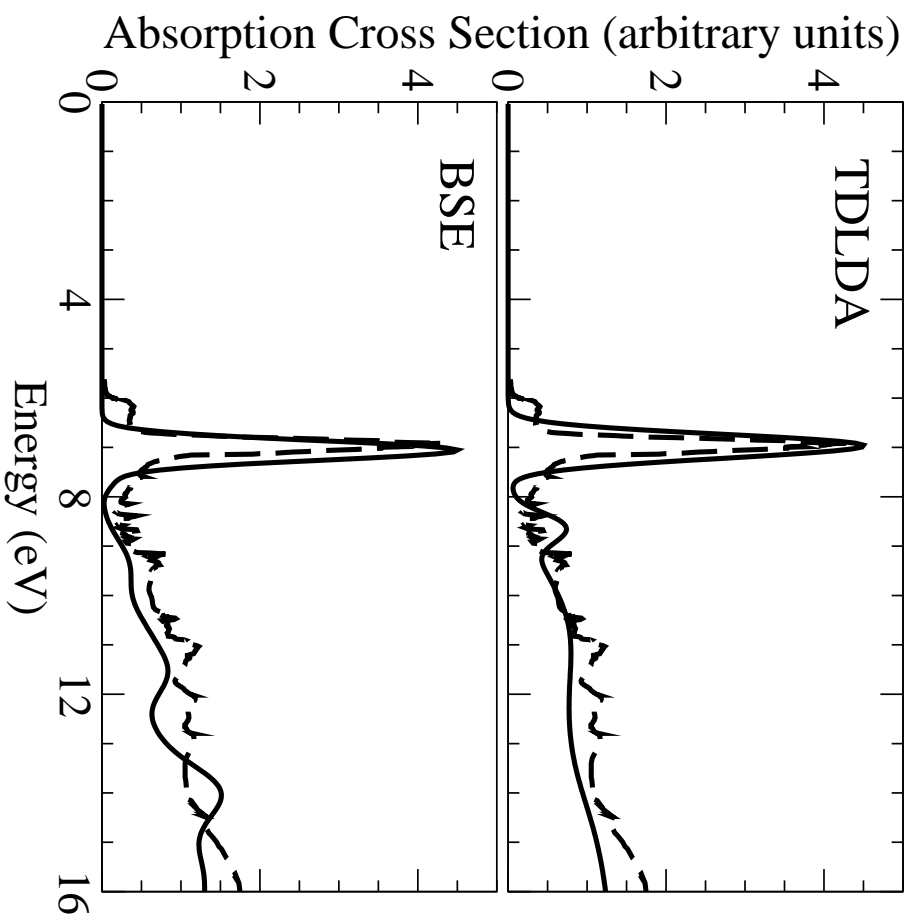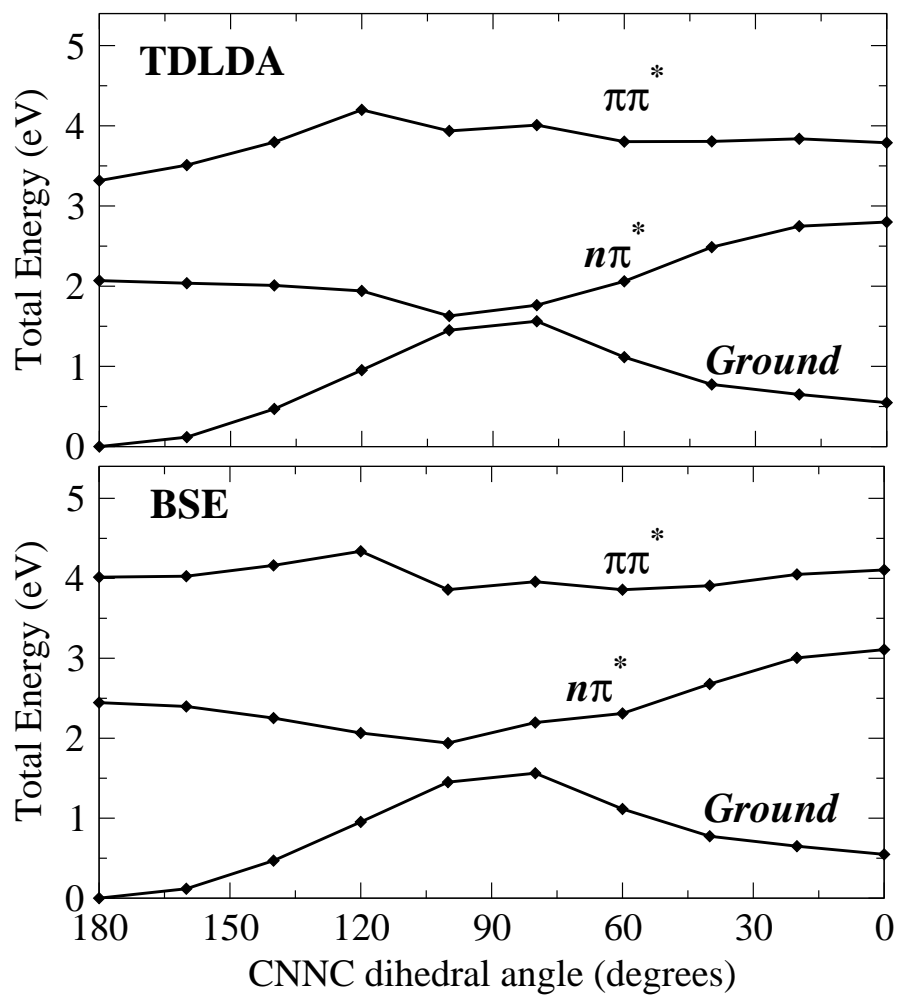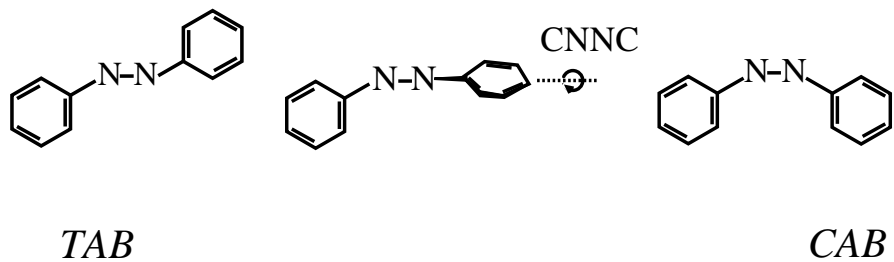
FIG. 1:

TAB   *CAB*

FIG. 2: